Adsorptive denitrogenation of model oil by Al-NDC@GO composites: Remarkable adsorption capacity and high selectivity

Xin Hu, Zareen Zuhra, Shafqat Ali, Yunshan Zhou*, Lijuan Zhang*, Xiaoya Duan, Zipeng Zhao
State Key Laboratory of Chemical Resource Engineering, Institute of Science, Beijing University of Chemical Technology, Beijing, 100029, P. R. China

Materials

The chemicals aluminum nitrate nonahydrate (analytical grade) and n-octane (analytical grade) were purchased from Tianjin Guangfu Technology Development Co. Ltd.; 1,4-naphthalenecarboxylic acid (1,4-H_2NDC, 98 %), methanol (HPLC grade), pyridine (PY, 99.8 %), indole (IND, 99 %) and quinoline (QUI, 99 %) were purchased from Beijing Chemical Reagent Co. Ltd. These reagents were used as obtained. The Al-NDC MOF material was prepared according to the published method [1].The graphene oxide (GO) was prepared with modified Hummer' method.[2]

Apparatus

The Fourier Transform Infrared spectra (FT-IR) were recorded on a Nicolet FTIR-170SX spectrometer with KBr pellets in the range of 400-4000 cm^{-1}. The powder X-ray diffraction (PXRD) data was collected on a Rigaku D/max 2500 X-ray diffractometer at a scanning rate of 10°/min in the 2θ range from 5° to 70° with graphite-monochromatic Cu K_α radiation (λ = 0.15405 nm). SEM images and EDX data were obtained using scanning electron microscope Zeiss Supra55 at an accelerating voltage of 20 kV. The nitrogen adsorption and desorption isotherms were measured at 77 K on an ASAP-2020 (Micrometrics USA). The specific surface area (S_{BET}) was determined from the linear part of the BET equation (P/P_0 = 0.05-0.3). The pore size distribution was derived from the desorption branch of the N_2 isotherm using the Barrett-Joyner-Halenda (BJH) method. The total pore volume was estimated from the amount of carbon dioxide adsorbed at a relative pressure (P/P_0) of ca. 0.99. The nitrogen contents of the model oils were analyzed by Agilent HPLC 1100 Series with C-18 column, diameter 4.6 mm, length 250 mm, diameter of filler 5 μm, 10 % water and 90 % methanol as the initial mobile phase, gradient elution to 100 % methanol in 10 min with flow rate of 1.0 mL min^{-1}**.**

Adsorption calculations

Adsorbed amount

All the adsorption capacities (mg/g) were calculated from the difference between final concentration and initial concentration of an adsorbate by using following equation:

$$q_t = \frac{(C_i - C_f)}{M} \quad \text{..... (Eq. S1)}$$

Where

q_t = adsorbed amount in time t (mg/g)

C_i = initial concentration of the adsorbate (mg/ml)

C_f = final concentration of the adsorbate (mg/ml)

V = volume of the solution subjected to a single adsorption (ml)

M = mass of the adsorbent taken during a single adsorption (g)

Maximum adsorption capacity

The maximum adsorption capacity (Q_o) was calculated using the Langmuir adsorption isotherm. The adsorption isotherms for different adsorbents were plotted according to the Langmuir equation [3]:

$$\frac{C_e}{q_e} = \frac{C_o}{Q_o} + \frac{1}{Q_o b} \quad \text{..... (Eq. S2)}$$

Where

C_e = the equilibrium concentration of the adsorbate (mg/L)

q_e = the amount adsorbed at the equilibrium (mg/g)

Q_o = the Langmuir constant (maximum adsorption capacity mg/g)

b = the Langmuir constant (L/mg)

Therefore, the maximum adsorption capacity, Q_o could be obtained from the reciprocal of the slope of a plot of C_e/q_e against C_e.

The separation factor (R_L) was calculated using the following equation that describes the adsorption process [4-7]:

$$R_L = \frac{1}{1 + bC_o} \quad \text{..... (Eq. S3)}$$

Where

R_L = separation factor

b = the Langmuir constant (L/mg)

C_o = initial concentration of adsorbate (mg/L)

Table S1. Comparison of the adsorptive denitrogenation capacities of different adsorbents in model oil system

Adsorbent	Type of NCCs	Q_o(mg- NCC/g)	Q_o (mg-N/g)	Reference
AC	quinoline, indole	-	39.0	[8, 9]

Cu-Y	NCCs with aromatic rings	-	3.0	[10, 11]
Silica- Alumina	Mixed	-	10.0	[12, 13]
Alumina	quinolene, indole	-	7.16	[14]
Meso-silica	Mixed	-	8.14	[15]
MOF (MIL-101)	Mixed	-	19.6	[16, 17]
MIL-100 (Cr)	quinoline, indole	445	49.4	[18]
PVDF/MIL-101	quinoline, indole	426	47.8	[19, 20]
NH_2-UiO-66	Indole	312	37.3	[21, 22]
Al-NDC@GO-4	Indole	487	61.2	This work
	Quinoline	670	72	This work
	Pyridine	533	86	This work

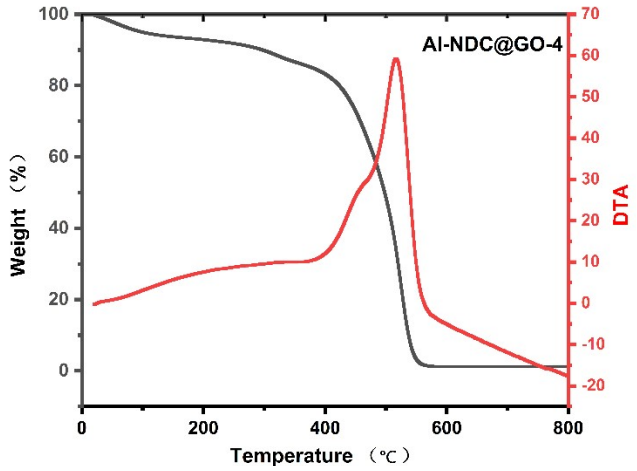

Fig.S1 TG-DTA patterns of Al-NDC@GO-4

Table S2. Fitting parameters of PY for Al-NDC and Al-NDC@GO-1/4 composites at different initial concentration

Model	ExpDec2
Equation	y = A1*exp(-x/t1) + A2*exp(-x/t2) + y0

Plot	Al-NDC@GO-4	Al-NDC	Al-NDC@GO-1
y0	9.59851E7 ± --	2859.01429 ± 1483.29052	287.32864 ± 508.63927
A1	-132.89031 ± 49.41997	-20.88941 ± 3.03868	-284.95494 ± 355.17732
t1	30.96496 ± 25.86062	61.94119 ± 20.73591	305.61258 ± 418.64164
A2	30.96496	-2832.46812 ± 1481.2534	16.933 ± 143.6156
t2	30.96496	15267.66607 ± 8475.76135	-427.31376 ± 1068.11579
Reduced Chi-Sqr	30.96496	0.6284	122.69596
Pearson's r	30.96496	0.99999	0.99924
Adj. R-Square	30.96496	0.99994	0.99619

Table S3. Fitting parameters of QUI for Al-NDC and Al-NDC@GO-1/4 composites at different initial concentration

Model	ExpDec2		
Equation	y = A1*exp(-x/t1) + A2*exp(-x/t2) + y0		
Plot	Al-NDC@GO-1	Al-NDC	Al-NDC@GO-4
y0	820.56574 ± 172.91105	371.63142 ± 0	1169.39033 ± 634.56375
A1	-798.89357 ± 162.5462	-185.81571 ± 0	-27.30787 ± 67.10747
t1	2543.15298 ± 833.10218	959.02428 ± 0	223.38163 ± 451.0617
A2	-22.27424 ± 15.81506	-185.81571 ± 0	-1140.76049 ± 568.32601
t2	52.66427 ± 112.15789	1172.14078 ± 0	3216.55229 ± 2689.66709
Reduced Chi-Sqr	86.68652	0	16.26822
Pearson's r	0.99891	0.98742	0.99977
Adj. R-Square	0.99745	0.99745	0.99946

Table S4. Fitting parameters of IND for Al-NDC and Al-NDC@GO-1/4 composites at different initial concentration

Model	ExpDec2		
Equation	y = A1*exp(-x/t1) + A2*exp(-x/t2) + y0		
Plot	Al-NDC	Al-NDC@GO-1	Al-NDC@GO-4
y0	395.91618 ± 139.80485	583.94769 ± 83.00155	600.36375 ± 57.53141
A1	-2.14043 ± 37.27259	-579.73485 ± 79.42152	-595.18313 ± 54.46682
t1	1.51164 ± 7.88388E10	546.96224 ± 118.63307	417.96561 ± 67.09795
A2	-382.4472 ± 118.38024	0.07714 ± 0.9534	0.10527 ± 0.85338
t2	1403.51059 ± 995.89359	-225.7381 ± 390.74799	-216.90134 ± 247.50623
Reduced Chi-Sqr	351.11986	140.50633	154.59956
Pearson's r	0.99397	0.9985	0.99862
Adj. R-Square	0.96983	0.9973	0.99752

Table S5. Langmuir fitting parameters of PY for Al-NDC and Al-NDC@GO-1/4 composites at different initial concentration

Equation	y = a + b*x
Weight	No Weighting

Residual Sum of Squares	1.74583	0.16018	0.15713
Pearson's r	0.90531	0.96252	0.95932
Adj. R-Square	0.77448	0.90806	0.90036
		Value	Standard Error
Al-NDC	Intercept	2.35314	0.39698
	Slope	0.00228	5.34735E-4
Al-NDC@GO-1	Intercept	0.78418	0.11527
	Slope	0.00147	2.0777E-4
Al-NDC@GO-4	Intercept	0.26721	0.10855
	Slope	0.0017	2.50102E-4

Table S6. Langmuir fitting parameters of IND for Al-NDC and Al-NDC@GO-1/4 composites at different initial concentration

Equation	y = a + b*x		
Weight	No Weighting		
Residual Sum of Squares	0.04548	0.51365	0.21979
Pearson's r	0.99843	0.9556	0.91378
Adj. R-Square	0.99528	0.8958	0.79373
		Value	Standard Error
Al-NDC	Intercept	2.06682	0.13327
	Slope	0.00218	8.64961E-5
Al-NDC@GO-1	Intercept	2.14348	0.18333
	Slope	0.00121	1.67089E-4
Al-NDC@GO-4	Intercept	1.92354	0.15212
	Slope	0.00117	2.59443E-4

Table S7. Langmuir fitting parameters of QUI for Al-NDC and Al-NDC@GO-1/4 composites at different initial concentration

Equation	y = a + b*x		
Weight	No Weighting		
Residual Sum of Squares	0.04548	0.51365	0.21979
Pearson's r	0.99843	0.9556	0.91378
Adj. R-Square	0.99528	0.8958	0.79373
		Value	Standard Error
Al-NDC	Intercept	2.06682	0.13327
	Slope	0.00218	8.64961E-5
Al-NDC@GO-1	Intercept	2.14348	0.18333
	Slope	0.00121	1.67089E-4
Al-NDC@GO-4	Intercept	1.92354	0.15212
	Slope	0.00117	2.59443E-4

References

1. A. Comotti, S. Bracco, P. Sozzani, S. Horike, R. Matsuda, J. Chen, M. Takata, Y. Kubota and S. Kitagawa, *J. Am. Chem. Soc.*, 2008, **130**, 13664-13672.
2. T. Chen, B. Zeng, J. L. Liu, J. H. Dong, X. Q. Liu, Z. Wu, X. Z. Yang and Z. M. Li, *J. Phys.:Conf. Ser.*, 2009, **188**, 012051.
3. Y. S. Ho and G. McKay, *Process Biochem.*, 1999, **34**, 451-465.
4. B. H. Hameed and A. A. Rahman, *J. Hazard. Mater.*, 2008, **160**, 576-581.
5. S. Lin and R. Juang, *J. Environ. Manage.*, 2009, **90**, 1336-1349.
6. K. P. Singh, D. Mohan, S. Sinha, G. S. Tondon and D. Gosh, *Ind. Eng. Chem. Res.*, 2003, **42**, 1965-1976.
7. Z. Ni, S. Xia, L. Wang, F. Xing and G. Pan, *J. Colloid Interf. Sci.*, 2007, **316**, 284-291.
8. Y. Hu, N. Li, J. Jiang, Y. Xu, X. Luo and J. Cao, *Front. Env. Sci. Eng.*, 2021, **16**, 90.
9. N. Li, M. Almarri, X. Ma and Q. Zha, *New Carbon Mater.*, 2011, **26**, 470-478.
10. P. J. Jodłowski, I. Czekaj, P. Stachurska, Ł. Kuterasiński, L. Chmielarz, R. J. Jędrzejczyk, P. Jeleń, M. Sitarz, S. Górecka, M. Mazur and I. Kurzydym, *Catalysts*, 2021, **11**, 824.
11. Y. Wu, J. Xiao, L. Wu, M. Chen, H. Xi, Z. Li and H. Wang, *J. Phys. Chem. C*, 2014, **118**, 22533-22543.
12. Q. Meng, A. Wang, C. Liu, E. Wang, A. Duan, Z. Zhao and G. Jiang, *Fuel*, 2022, **326**, 125084.
13. Y. Bae, M. Kim, H. Lee, C. Lee and J. Ryu, *AlChE J.*, 2006, **52**, 510-521.
14. X. Wei, J. Miao, Z. Lv, X. Wan, N. Zhang, R. Zhang and S. Peng, *Appl. Sci.*, 2022, **12**, 2309.
15. J. You, H. Song, J. Zhang, C. Chen and F. Han, *Fuel*, 2019, **241**, 997-1007.
16. I. Ahmed, N. A. Khan and S. H. Jhung, *Inorg. Chem.*, 2013, **52**, 14155-14161.
17. M. M. H. Mondol, B. N. Bhadra, J. M. Park and S. H. Jhung, *Chem. Eng. J.*, 2021, **404**, 126491.
18. M. Songolzadeh, M. Soleimani and M. Takht Ravanchi, *Micropor. Mesopor. Mat.*, 2019, **274**, 54-60.
19. I. Ahmed, N. A. Khan, Z. Hasan and S. H. Jhung, *J. Hazard. Mater.*, 2013, **250-251**, 37-44.
20. L. Ni, Y. Zhu, J. Ma and Y. Wang, *Water Res.*, 2021, **188**, 116554.
21. G. W. Peterson, J. J. Mahle, J. B. DeCoste, W. O. Gordon and J. A. Rossin, *Angew.Chem.Int.Edit.*, 2016, **55**, 6235-6238.
22. H. Fakhri, A. Esrafili, M. Farzadkia, R. Boukherroub, V. Srivastava and M. Sillanpää, *New J. Chem.*, 2021, **45**, 10897-10906.